medRxiv preprint doi: https://doi.org/10.1101/2022.09.27.22280379; this version posted September 27, 2022. The copyright holder for this preprint (which was not certified by peer review) is the author/funder, who has granted medRxiv a license to display the preprint in perpetuity. All rights reserved. No reuse allowed without permission.

Amyloid and Tau Pathology are Associated with Cerebral Blood Flow in Nondemented Older Adults with and without Vascular Risk Factors for Alzheimer's Disease

Cecily G. Swinford[a,b], Shannon L. Risacher[a,b], Aaron Vosmeier[a,b], Rachael Deardorff[a,b], Evgeny J. Chumin[b,e,f], Mario Dzemidzic[b,d], Yu-Chien Wu[a,b], Sujuan Gao[b,g], Brenna C. McDonald[a,b,d], Karmen K. Yoder[a,b], Frederick W. Unverzagt[b,h], Sophia Wang[b,h], Martin R. Farlow[b,d], Jared R. Brosch[b,d], David G. Clark[b,d], Liana G. Apostolova[a,b,d,e], Justin Sims[a], Danny J. Wang[c], and Andrew J. Saykin[a,b,d,e]

Author Affiliations:

a) Department of Radiology and Imaging Sciences, Indiana University School of Medicine, 355 W. 16th Street, Goodman Hall, Suite 4100, Indianapolis, IN 46202
b) Indiana Alzheimer's Disease Research Center, 355 W. 16th Street, Goodman Hall, Suite 4100, Indianapolis, IN 46202
c) Stevens Neuroimaging and Informatics Institute, Keck School of Medicine of University of Southern California, SHN 2025 Zonal Ave. Los Angeles, CA 90033
d) Department of Neurology, Indiana University School of Medicine, 355 W. 16th Street Goodman Hall Suite 4700, Indianapolis, IN 46202
e) Indiana University Network Science Institute, 1015 E. 11th Street, Bloomington, IN 47408
f) Department of Psychological and Brain Sciences, Indiana University, 1101 E. 10th Street, Bloomington, IN 47405
g) Department of Biostatistics and Health Data Sciences, Indiana University School of Medicine, 410 W. 10th Street HITS 3000, Indianapolis, IN 46202
h) Department of Psychiatry, Indiana University School of Medicine, 355 W. 16th Street Goodman Hall, Indianapolis, IN 46202

Author Email Addresses: cgswinfo@iupui.edu, srisache@iupui.edu, aavosm@iu.edu, radear@iu.edu, echumin@iu.edu, mdzemidz@iupui.edu, yucwu@iu.edu, sgao@iu.edu, mcdonalb@iupui.edu, kkyoder@iupui.edu, funverza@iu.edu, sophwang@iupui.edu, mfarlow@iupui.edu, jbrosch@iupui.edu, clarkdg@iu.edu, lapostol@iu.edu, simsjb@iupui.edu, dannyjwa@usc.edu, asaykin@iupui.edu

Corresponding Author: Andrew J. Saykin
Email: asaykin@iupui.edu
Address: 355 W. 16th Street GH Suite 4100, Indianapolis, IN 46202

NOTE: This preprint reports new research that has not been certified by peer review and should not be used to guide clinical practice.

medRxiv preprint doi: https://doi.org/10.1101/2022.09.27.22280379; this version posted September 27, 2022. The copyright holder for this preprint (which was not certified by peer review) is the author/funder, who has granted medRxiv a license to display the preprint in perpetuity. All rights reserved. No reuse allowed without permission.

Abstract

Alzheimer's disease (AD) is the leading cause of dementia in individuals over 65 in the U.S. Prevalence is projected to double by 2050, but current treatments cannot stop the progression of AD. Treatments administered before severe cognitive decline may be effective; identification of biomarkers for preclinical/prodromal stages of AD is therefore imperative. Cerebral blood flow (CBF) is a potential early biomarker for AD; generally, older adults with AD have decreased CBF compared to normally aging peers. Characterization should include the relationship between CBF and AD risk factors and pathologies. We assessed the relationships between CBF quantified by arterial spin labeled MRI, hypertension, *APOE* ε4, and amyloid and tau PET in 78 older adults: cognitively normal, subjective cognitive decline, and mild cognitive impairment. Decreased regional CBF was associated with increased tau pathology, and the relationship between CBF and amyloid pathology differed by hypertension status. Our findings suggest a complex relationship between risk factors, AD pathologies, and CBF that warrants future studies of CBF as a potential early biomarker for AD.

Keywords: tau PET, amyloid PET, cerebral blood flow, arterial spin labeled MRI, biomarkers, mild cognitive impairment

Funding: This study was funded in part by the following grants from the National Institute on Aging: K01 AG049050, R01 AG061788, P30 AG010133, P30 AG072976, R01 AG019771, R01 AG057739, U01 AG024904, R01 AG068193, T32 AG071444, U01 AG068057, and U01 AG072177 and the National Library of Medicine: R01 LM013463. In kind support for tau PET tracer precursor was provided by Avid Radiopharmaceuticals, a subsidiary of Eli Lilly and Company.

medRxiv preprint doi: https://doi.org/10.1101/2022.09.27.22280379; this version posted September 27, 2022. The copyright holder for this preprint (which was not certified by peer review) is the author/funder, who has granted medRxiv a license to display the preprint in perpetuity. All rights reserved. No reuse allowed without permission.

1. Introduction

Alzheimer's disease (AD)[1] is the leading cause of dementia; over 6 million older adults in the U.S. have AD, and this number is projected to double over the next thirty years (Alzheimer's Disease Facts and Figures, 2021). The results of multiple studies and clinical trials suggest that an effective treatment for AD will likely need to be preventative (Jessen et al., 2014; Crous-Bou et al., 2017). Although there are some promising exceptions, treatments targeting amyloid and tau pathology administered after the emergence of clinical symptoms have generally been unable to restore cognitive function (Lu et al., 2020; Congdon and Sigurdsson, 2018). Therefore, it is imperative to find reliable and accurate biomarkers for the earliest, preclinical stages of AD in order to identify individuals who would benefit from preventative treatment. One such potential early biomarker is quantitative cerebral blood flow (CBF).

CBF is known to be decreased in individuals with AD compared to healthy individuals of the same age (Alsop et al., 2000). This decrease has also been shown to be more than would be expected given the amount of brain atrophy in these individuals, suggesting that altered CBF is itself a pathologic phenomenon in AD (Binnewijzend et al., 2013). These results have led to the development of the two-hit hypothesis of AD, which posits that vascular risk factors and amyloid accumulation exacerbate one another and eventually lead to tau aggregation, neurodegeneration, and cognitive decline (Zlokovic, 2011; Korte et al., 2020). This differs from the longstanding amyloid cascade hypothesis, which posits that amyloid deposition triggers the onset and

[1] Abbreviations: Aβ – amyloid beta, AAL – Automated Anatomical Labeling, AD – Alzheimer's disease, ADNI – Alzheimer's Disease Neuroimaging Initiative, APOE – apolipoprotein E, ANCOVA – analysis of covariance, ANOVA – analysis of variance, ASL – arterial spin labeled, CBF – cerebral blood flow, CCI – Cognitive Change Index, CN – cognitively normal, CSF – cerebrospinal fluid, FWE – Family-Wise Error, FWHM – full width at half maximum, MCI – mild cognitive impairment, MNI – Montreal Neurological Institute, MRI – magnetic resonance imaging, MTL – medial temporal lobe, pCASL – psuedocontinuous arterial spin labeled, PET – positron emission tomography, PIB – Pittsburgh compound B, ROI – region of interest, SCD – subjective cognitive decline, SPM – Statistical Parametric Mapping, SPSS – Statistical Package for the Social Sciences, SUVR – standardized uptake value ratio

medRxiv preprint doi: https://doi.org/10.1101/2022.09.27.22280379; this version posted September 27, 2022. The copyright holder for this preprint (which was not certified by peer review) is the author/funder, who has granted medRxiv a license to display the preprint in perpetuity. All rights reserved. No reuse allowed without permission.

propagation of the complex pathologies and symptoms that comprise AD (Hardy and Higgins, 1992). Evidence for the two-hit model of AD includes the fact that vascular risk factors like hypertension, diabetes mellitus, and obesity are also risk factors for AD (Gorelick, 2004). Chronic hypertension, in particular, has been shown to cause cerebral microvascular damage, which both worsens and is worsened by amyloid beta (Aβ) aggregation. It has been suggested that altered CBF may occur very early in the course of AD, before cognitive symptoms and potentially even prior to amyloid and tau aggregation (Iadecola, 2004). Given that this early alteration of CBF may play a role in initiating the cascade of pathological changes culminating in AD, it is an intriguing potential early biomarker.

While altered CBF has been described as one of the earliest changes in AD, its typical spatial and temporal patterns throughout the disease course are not yet fully characterized. It has been shown that CBF increases in some brain regions in individuals on the AD spectrum, especially in preclinical and prodromal AD, known as subjective cognitive decline (SCD) and mild cognitive impairment (MCI) (Beishon et al., 2017; Dai et al., 2009). Altered CBF is largely characterized by hypoperfusion by the time individuals have some level of cognitive decline (Wierenga et al., 2014; Swinford et al., 2022). Increased CBF in early, preclinical stages may be compensatory in response to other AD-related pathologies, like amyloid or tau aggregation. Indeed, global CBF is positively correlated with cognitive test scores (Boles et al., 2006). Vascular risk factors such as hypertension and genetic risk factors including the apolipoprotein E (*APOE)* ε4 allele may play a role in whether individuals have a compensatory increase in CBF and for how long that compensation can be maintained despite pathology and vascular dysfunction. It is also important to elucidate the spatial and temporal relationships between altered CBF and other AD-related pathologies, including amyloid and tau aggregation. CBF

medRxiv preprint doi: https://doi.org/10.1101/2022.09.27.22280379; this version posted September 27, 2022. The copyright holder for this preprint (which was not certified by peer review) is the author/funder, who has granted medRxiv a license to display the preprint in perpetuity. All rights reserved. No reuse allowed without permission.

tends to be negatively correlated with both amyloid and tau pathology (Albrecht et al., 2020; Rubinski et al., 2021; Visser et al., 2020; Mattsson et al., 2014; Rodell et al., 2016; Tosun et al., 2016); however, some studies also report positive correlations between CBF and these pathologies, mostly in individuals with preclinical AD (Codispoti et al., 2012; Stomrud et al., 2012; Fazlollahi et al., 2020; Tosun et al., 2014; Sojkova et al., 2008). It has been established that both hypertension and *APOE* ε4 positivity are related to increased Aβ aggregation and are associated with cerebrovascular dysfunction and decreased CBF (Solis et al., 2020; Bell et al., 2012; Wiesmann et al., 2016). In this study, we aimed to assess the relationships between CBF and amyloid and tau pathologies in older nondemented adults and to determine whether the presence of the *APOE* ε4 allele and/or hypertension affects those relationships.

Extensive characterization of altered CBF in the context of preclinical AD is necessary to establish it as an effective early biomarker. In older nondemented adults, we assessed the relationships between CBF and global cortical amyloid and medial temporal lobe (MTL) tau pathology using arterial spin labeled (ASL) magnetic resonance imaging (MRI) and positron emission tomography (PET), as well as the interaction effects of *APOE* ε4 positivity and hypertension on the relationship of CBF with amyloid and tau. We hypothesized that amyloid and tau pathologies would negatively correlate with CBF overall, although localized regions of positive correlation would be present as well, given the early stage of disease in this sample. We also hypothesized that individuals with hypertension or at least one *APOE* ε4 allele would be less likely to have a compensatory positive correlation between CBF and AD-related pathologies.

2. Methods

2.1 Participants

medRxiv preprint doi: https://doi.org/10.1101/2022.09.27.22280379; this version posted September 27, 2022. The copyright holder for this preprint (which was not certified by peer review) is the author/funder, who has granted medRxiv a license to display the preprint in perpetuity. All rights reserved. No reuse allowed without permission.

This study included 78 participants (30 cognitively normal [CN], 25 SCD, 23 MCI) from the Indiana Alzheimer's Disease Research Center who were at least sixty years of age. All participants completed T1-weighted structural and pseudocontinuous arterial spin labeled (pCASL) MRI scans, amyloid PET scan with either [^{18}F]florbetapir or [^{18}F]florbetaben, and tau PET scan with [^{18}F]flortaucipir. All participants also had a clinical assessment and *APOE* genotyping. Diagnoses were determined by clinician consensus. SCD was defined as a score of 20 or more on the first 12 items of the 20-item Cognitive Change Index (CCI-20; Saykin et al., 2006), reflecting increased subjective memory concerns, with or without increased levels of informant-based concerns (Jessen et al., 2014), and the absence of a measurable cognitive deficit on objective cognitive assessment. Using standard criteria, an individual was diagnosed with MCI if the participant and/or an informant had a significant complaint about their cognition, and the participant scored 1.5 standard deviations or more below age-, education-, and sex-adjusted normative data on objective tests of cognitive functioning, either in memory or another cognitive domain. Additionally, individuals diagnosed with MCI, by definition, do not show a significant decline in daily functioning. Hypertension was defined by self-report near the time of imaging. Individuals defined as hypertensive reported a previous diagnosis of hypertension. Some hypertensive individuals were taking antihypertensive medication at the time of the study. All procedures were approved by the Indiana University School of Medicine Institutional Review Board. Informed consent was obtained according to the Declaration of Helsinki and the Belmont Report.

2.2 pCASL and T1-weighted MRI

medRxiv preprint doi: https://doi.org/10.1101/2022.09.27.22280379; this version posted September 27, 2022. The copyright holder for this preprint (which was not certified by peer review) is the author/funder, who has granted medRxiv a license to display the preprint in perpetuity. All rights reserved. No reuse allowed without permission.

All MRI scans were acquired on the same Siemens 3T Prisma scanner with a 64-channel head/neck radiofrequency coil. After an initial T1-weighted structural scan (sagittal 3D MPRAGE) each participant completed a 3D pseudo-continuous ASL (pCASL) MRI scan. The full MRI protocol consisted of MPRAGE, FLAIR, high resolution hippocampus imaging, DTI, fMRI, HYDI DTI, pCASL, and finally SWI over a total of roughly 58 minutes. The MPRAGE scan had the following parameters: repetition time (TR) 2300 ms, echo time (TE) 2.95 ms, field of view 270 mm, 176 slices, and voxel size 1.1 x 1.1 x 1.2 mm^3. The pCASL scan was acquired with Fair QII using a multi-slice interleaved saturation sequence with the following parameters: repetition time (TR) 3840 ms, echo time (TE) 40.7 ms, field of view 240 mm x 240 mm, 54 slices with 2.5 mm thickness, image matrix 96 x 96, and voxel size 2.5 x 2.5 x 2.5 mm^3. The label duration was 1500ms and post-labeling delay (PLD) was 1800ms. The total acquisition time was 7min 18sec including a M0 image and 7 pairs of label and control images.

Processing steps were performed using Statistical Parametric Mapping 12 (SPM12; Wellcome Department of Cognitive Neuroscience, London, UK) and Matlab R2022a as previously described (Butcher et al., 2021; Wang et al., 2003). For each individual, all pCASL images were aligned to the first pCASL image and averaged. The mean pCASL image was coregistered to the individual's structural MRI image, and the structural image was coregistered to an averaged brain mask template. Then to obtain gray matter maps, the individual T1-weighted structural MRI images were segmented, and the gray matter images were normalized and smoothed with a 6 mm isotropic full width at half maximum (FWHM) Gaussian kernel. To calculate CBF from pCASL images, pairs of pCASL images were subtracted and then averaged to obtain a mean perfusion image. A standard single-compartment perfusion model (Alsop et al., 2015) was used to calculate mean CBF maps from the mean perfusion images

medRxiv preprint doi: https://doi.org/10.1101/2022.09.27.22280379; this version posted September 27, 2022. The copyright holder for this preprint (which was not certified by peer review) is the author/funder, who has granted medRxiv a license to display the preprint in perpetuity. All rights reserved. No reuse allowed without permission.

(http://cfn.upenn.edu/perfusion/software.htm). To create a gray matter mask, the gray matter tissue map from the SPM12-segmented structural MRI was coregistered to the mean perfusion image, thresholded (> 0.75), smoothed (isotropic 6 mm FWHM Gaussian kernel), and binarized (> 0.20). This individualized gray matter mask was then applied to the mean CBF map, which was normalized to Montreal Neurological Institute (MNI) atlas space using nonlinear transformation parameters from the segmentation step, resampled to 2 mm/side isotropic voxels, and smoothed with an isotropic 6 mm FWHM Gaussian kernel, with the cerebellum excluded in order to remove individual variability in this region due to the imaging method. CBF was extracted from the resulting masked CBF map from frontal, parietal, temporal, and occipital lobes and limbic regions of interest (ROIs) using Automated Anatomical Labeling (AAL) version 1 and the MarsBaR toolbox (Brett et al., 2002).

2.3 Amyloid PET

Each participant underwent either a [^{18}F]florbetapir (AmyVid; Eli Lilly and Co.) or a [^{18}F]florbetaben (Neuraceq; Life Molecular Imaging, formerly Piramal Imaging) scan. For the [^{18}F]florbetapir scans, 10 mCi $\pm$ 10% of [^{18}F]florbetapir was injected intravenously, followed by a 50-minute uptake period. For [^{18}F]florbetaben scans, 8.1 mCi $\pm$ 10% of [^{18}F]florbetaben was injected intravenously, followed by a 90-minute uptake period. Participants were then imaged on the same Siemens Biograph mCT PET/CT scanner for 20 minutes with continuous list mode data acquisition. For both types of scans, a computed tomography scan was acquired for scatter and attenuation correction. The list mode data were then binned into four 5-minute frames and reconstructed using parameters defined in the Alzheimer's Disease Neuroimaging Initiative (ADNI) protocol (http://adni.loni.usc.edu). These parameters include corrections for scatter and

medRxiv preprint doi: https://doi.org/10.1101/2022.09.27.22280379; this version posted September 27, 2022. The copyright holder for this preprint (which was not certified by peer review) is the author/funder, who has granted medRxiv a license to display the preprint in perpetuity. All rights reserved. No reuse allowed without permission.

random coincidence events, attenuation, and radionuclide decay. Each 5-minute frame was spatially aligned to the participant's T1-weighted structural MRI using coreg, normalized to MNI space, and smoothed with an 8 mm FWHM Gaussian kernel, all using SPM12. The spatially aligned PET images were averaged to create a single image from the total acquisition time period for each individual (50-70 minutes for [^{18}F]florbetapir and 90-110 minutes for [^{18}F]florbetaben), and standardized uptake value ratio (SUVR) images were generated by intensity normalizing with the average radioactivity from a whole cerebellar region of interest from the Centiloid project (http://www.gaain.org/Centiloid-project/). For this study, we used the global cortical amyloid measure calculated in Centiloid units, a unified metric that allowed us to directly compare data from both scan types. The global cortical ROI was determined by the Centiloid project and is the ROI for which use of Centiloid units is intended. Both types of scans were processed with the Centiloid algorithm at a voxel-wise level as defined by the Centiloid project (Risacher et al., 2021). Global cortical Centiloid data were then extracted from both scan types using the MarsBaR toolbox (Brett et al., 2002). Amyloid positivity was defined as global cortical amyloid >21 Centiloid units.

2.4 Tau PET

All participants underwent a [^{18}F]flortaucipir PET scan. 10 mCi $\pm$ 10% of [^{18}F]flortaucipir was injected intravenously, followed by a 75-minute uptake period. Individuals were then imaged on the same Siemens Biograph mCT PET/CT scanner for 30 minutes with continuous list mode data acquisition. These data were binned into six 5-minute frames, and scans were reconstructed using a standard scanner software program (Siemens, Knoxville, TN) according to the ADNI protocol (http://adni.loni.usc.edu). The 5-minute frames corresponding to

medRxiv preprint doi: https://doi.org/10.1101/2022.09.27.22280379; this version posted September 27, 2022. The copyright holder for this preprint (which was not certified by peer review) is the author/funder, who has granted medRxiv a license to display the preprint in perpetuity. All rights reserved. No reuse allowed without permission.

80-100 minutes post-injection were spatially aligned to each participant's T1 image and normalized to MNI space, averaged to create a single image, intensity normalized by the cerebellar crus (Schwarz et. al., 2016) to create SUVR images, and smoothed with an 8 mm FWHM Gaussian kernel, all using SPM12. For this study, we extracted the MTL SUVR. The constituent ROIs were generated from FreeSurfer 6.0 (Fischl and Dale, 2000; http://surfer.nmr.mgh.harvard.edu/), and the bilateral mean MTL (average of fusiform gyri, parahippocampal gyri, and entorhinal cortex) SUVR values were extracted for each participant using MarsBaR. For interaction analyses, tau positivity was defined as MTL tau SUVR greater than the third quartile value in this sample (1.152). This relative definition of tau positivity was similar to a previous data-driven tau cutoff (Mishra et. al., 2017).

2.5 Statistical Analyses

The demographic and clinical variables, as well as global CBF, total gray matter volume, and amyloid and tau PET measures were compared between diagnostic groups using one-way ANOVA for continuous variables and chi-square test for categorical variables. Stepwise multiple regression model (entry p=0.10, removal p=0.20) with dependent variable regional CBF and independent variables diagnostic group, age, sex, hypertension status, *APOE* ε4 status, and total gray matter volume (from T1-weighted image gray matter estimates by SPM12 tissue volume utility) were used to determine demographic/clinical variables that correlated with CBF in this sample. Additionally, amyloid and tau PET metrics were treated as the dependent variables in a multiple regression model with age, sex, hypertension status, *APOE* ε4 status, and total gray matter volume as independent variables to assess correlations between amyloid and tau PET and demographic/clinical variables. Partial Pearson correlations assessed the relationship between

medRxiv preprint doi: https://doi.org/10.1101/2022.09.27.22280379; this version posted September 27, 2022. The copyright holder for this preprint (which was not certified by peer review) is the author/funder, who has granted medRxiv a license to display the preprint in perpetuity. All rights reserved. No reuse allowed without permission.

regional CBF and amyloid or tau PET metrics, with age, sex, total gray matter volume, hypertension status, and *APOE* ε4 status as covariates. Analyses including CBF were repeated on a voxel-wise basis using multiple regression with CBF maps as the dependent variable and amyloid or tau PET metrics, age, sex, total gray matter volume, and hypertension status as independent variables or covariates as appropriate. A voxel-wise two-way ANCOVA model assessed interactions of amyloid/tau positivity and hypertension/*APOE* ε4 status with age, sex, and total gray matter volume as covariates. CBF was extracted from significant clusters and modeled as the dependent variable in linear regression to visualize interactions. Results are listed for clusters present when viewed at threshold $p \leq 0.001$, cluster size (k)≥50 voxels (uncorrected), significant at cluster-wise $p \leq 0.05$ with Family-Wise Error (FWE) correction, and with peak voxels within gray matter regions. All voxel-wise analyses were completed using SPM12. Other statistical analyses and all graphs were created in IBM SPSS 25.

3. Results

3.1 Demographics

Demographics and clinical variables are given in Table 1. The MCI group had a greater global cortical Centiloid value than the CN and SCD groups (p=0.001). Diagnostic groups also differed by prevalence of hypertension (p<0.001); the SCD group had the highest prevalence of hypertension, followed by MCI, and then by CN. Finally, the groups differed by proportion of women (p=0.05). CN had the greatest proportion of women, followed by SCD, and then by MCI. Global CBF did not differ by diagnostic group (p>0.6).

3.2 CBF vs. Demographics

medRxiv preprint doi: https://doi.org/10.1101/2022.09.27.22280379; this version posted September 27, 2022. The copyright holder for this preprint (which was not certified by peer review) is the author/funder, who has granted medRxiv a license to display the preprint in perpetuity. All rights reserved. No reuse allowed without permission.

Mean CBF from each lobe ROI was entered into a stepwise multiple regression with diagnosis, age, sex, hypertension status, *APOE* ε4 status, and total gray matter volume as independent variables. Age and hypertension were negatively correlated with CBF in all lobes (Table 2). No correlations were found between CBF and diagnosis, *APOE* ε4 status, or total gray matter volume. The age by hypertension status interaction was not statistically significant in any of the lobes. Voxel-wise regressions were used to model the spatial relationships between CBF and age (Figure 1A & B) and hypertension (Figure 1C & D) with covariates of sex, gray matter volume, and age where appropriate. Clusters and peak voxels for these correlations are presented in Tables 3 and 4.

3.3 Tau and Amyloid PET vs. Demographics

The global cortical Centiloid and the MTL tau SUVR data were used as dependent variables in a stepwise regression model with age, sex, hypertension status, *APOE* ε4 status, and total gray matter volume as independent variables. The global cortical Centiloid value was associated with *APOE* ε4 status (β=0.414, t=3.96, p<0.001). MTL tau SUVR was negatively associated with hypertension status (β=−0.223, t=−2.00, p=0.049).

3.4 Tau PET vs. Regional CBF

Partial correlations were completed for regional CBF with MTL tau SUVR, with age, sex, and total gray matter volume as covariates. There were no significant correlations for any of the ROIs between CBF and MTL tau SUVR. The addition of hypertension status and *APOE* ε4 status as covariates did not change the results. Using voxel-wise regression models with age, sex, and total gray matter volume as covariates, MTL tau SUVR was negatively correlated with CBF

medRxiv preprint doi: https://doi.org/10.1101/2022.09.27.22280379; this version posted September 27, 2022. The copyright holder for this preprint (which was not certified by peer review) is the author/funder, who has granted medRxiv a license to display the preprint in perpetuity. All rights reserved. No reuse allowed without permission.

in the left hippocampus and left parahippocampal gyrus ($p \leq 0.001$, $k \geq 50$; Table 5). The significant cluster and beta maps of the negative correlations between MTL tau SUVR and CBF are illustrated by Figure 2, and the partial correlation in the significant cluster ($R^2=0.256$) is plotted in Figure 3. In order to determine whether *APOE* ε4 status or hypertension status affected the relationship between amyloid or tau PET measures and CBF, a voxel-wise two-way ANCOVA was used, with CBF as the dependent variable, tau positivity and *APOE* ε4 or hypertension status as independent variables, and age, sex, and total gray matter volume as covariates. Tau positivity was defined as MTL tau SUVR greater than the third quartile value in this sample (mean: 1.110, SD: 0.110, range: 0.706, third quartile: 1.152). There were no effects of tau positivity by hypertension interaction or tau positivity by *APOE* ε4 positivity interaction on CBF.

3.5 Amyloid PET vs. Regional CBF

Partial correlations were completed for regional CBF with global cortical Centiloid, with age, sex, and total gray matter volume as covariates. There were no significant correlations for any of the ROIs between CBF and global cortical Centiloid. The addition of hypertension status and *APOE* ε4 status as covariates did not change the results. Using voxel-wise regression models with age, sex, and total gray matter volume as covariates, there were no statistically significant correlations between CBF and global cortical Centiloid at the $p \leq 0.001$, $k \geq 50$ level. In order to determine whether *APOE* ε4 status or hypertension status affected the relationship between amyloid or tau PET measures and CBF, a voxel-wise two-way ANCOVA was used, with CBF as the dependent variable, amyloid positivity and *APOE* ε4 or hypertension status as independent variables, and age, sex, and total gray matter volume as covariates. There was a positive

medRxiv preprint doi: https://doi.org/10.1101/2022.09.27.22280379; this version posted September 27, 2022. The copyright holder for this preprint (which was not certified by peer review) is the author/funder, who has granted medRxiv a license to display the preprint in perpetuity. All rights reserved. No reuse allowed without permission.

interaction of the amyloid positivity by hypertension interaction on cluster-wise CBF at $p \leq 0.001$, $k \geq 50$ (Table 6). Spatial patterns of the positive association between the interaction variable and CBF are illustrated by beta maps in Figure 4. CBF in the left visual motor area was positively associated with global cortical Centiloid in hypertensive individuals (R^2=0.200) and negatively associated with global cortical Centiloid in normotensive individuals (R^2=0.167; Figure 5). Each participant's CBF values from the significant cluster were extracted and entered into a regression model as the dependent variable with global cortical Centiloid, hypertension status, age, sex, total gray matter volume, and hypertension status by global cortical Centiloid interaction as independent variables. The interaction variable was positively associated with the cluster CBF (β=0.624, t=4.16, p<0.001), while global cortical Centiloid and hypertension were both negatively associated with the cluster CBF. There was no amyloid positivity by *APOE* ε4 positivity interaction effect on CBF.

4. Discussion

We found that CBF is negatively correlated with MTL tau aggregation in older adults. There was also an interaction effect of global cortical amyloid and hypertension status on CBF in this sample, where global cortical amyloid and CBF were positively correlated in hypertensive individuals and negatively correlated in normotensive individuals. Negative correlations between CBF and MTL tau aggregation were present in the parahippocampal gyrus and hippocampus.

Previous studies concerning the relationship between tau and CBF have reported negative correlations. Unlike amyloid pathology, tau tracks both spatially and temporally with disease severity and brain dysfunction. Therefore, as tau pathology progresses in its characteristic pattern over the disease course, lower CBF progresses similarly (Gomez-Isla et al., 1997; Ashford et al.,

medRxiv preprint doi: https://doi.org/10.1101/2022.09.27.22280379; this version posted September 27, 2022. The copyright holder for this preprint (which was not certified by peer review) is the author/funder, who has granted medRxiv a license to display the preprint in perpetuity. All rights reserved. No reuse allowed without permission.

2000). Similar to the amyloid literature, animal models of hypoperfusion develop increased tau pathology (Raz et al., 2019; Zhang et al., 2010), and animal models of tau pathology develop hypoperfusion (Bennett et al., 2018; Jaworski et al., 2011; Lourenco et al., 2017; Park et al., 2020). In human studies including either a mix of diagnoses including clinical AD or only clinical AD, there have been findings of negative correlations between tau pathology and CBF in temporal, parietal, and occipital lobes, and entorhinal cortex (Albrecht et al., 2020; Rubinski et al., 2021; Visser et al., 2020). Okamura et al. (2002) reported that the ratio of (increased) tau in cerebrospinal fluid (CSF) to (decreased) posterior cingulate CBF predicted the progression from MCI to AD with 88.5% sensitivity and 90% specificity. Studies in CN individuals report a mix of results, similar to amyloid pathology studies in preclinical AD. Hays et al. (2020) reported a negative correlation between CSF tau and CBF in the anterior cingulate cortex. Stomrud et al. (2012) reported a negative correlation between CSF tau and CBF in the medial frontal lobe, as well as a positive correlation between tau and CBF in the frontotemporal border zone. Another study reported that asymptomatic individuals with the same amount of tau pathology as individuals with MCI had increased CBF in the MTL and thalamus over time (Codispoti et al., 2012). Although there are fewer studies focused on the relationship between tau pathology and CBF compared to amyloid pathology, it appears that a similar pattern of findings is emerging.

Here, we found that MTL CBF correlates negatively with MTL tau pathology. These findings agree with previous reports of negative correlations between CBF and AD pathology in preclinical AD. They also agree with evidence of the temporal and spatial correlation between tau pathology and brain dysfunction in AD. While we did not see positive correlations between CBF and amyloid or tau pathology in the whole sample, as have also been reported in preclinical populations, this may be due to a limited sample size. There also may be distinct time courses for

medRxiv preprint doi: https://doi.org/10.1101/2022.09.27.22280379; this version posted September 27, 2022. The copyright holder for this preprint (which was not certified by peer review) is the author/funder, who has granted medRxiv a license to display the preprint in perpetuity. All rights reserved. No reuse allowed without permission.

compensation in response to Aβ and tau pathology that are dependent on other pathologies and risk factors. We also found that hypertension was associated with decreased CBF in this sample. This has been reported previously (Alosco et al., 2013). It has been described that chronic hypertension shifts microvascular regulation in favor of constriction, which leads to decreased CBF in hypertensive individuals (Toth et al., 2017). As the two-hit hypothesis of AD posits, vascular risk factors such as hypertension result in cerebrovascular dysfunction that both aggravates and is aggravated by amyloid and tau pathology.

Interacting relationships among multiple risk factors and pathologies in AD have been previously studied; specifically, the effect of *APOE* ε4 on relationships between CBF and other AD pathologies or symptoms has been reported. Two papers (Wang et al., 2019; Zlatar et al., 2016) reported a positive correlation between CBF and cognition in *APOE* ε4-negative CN individuals and a negative correlation between CBF and cognition in *APOE* ε4-positive CN individuals. Hays et al. (2020) found a negative relationship between tau in the cerebrospinal fluid and CBF in the anterior cingulate in *APOE* ε4-positive but not *APOE* ε4-negative individuals. *APOE* ε4 may act either alongside or synergistically with Aβ to exacerbate neurodegeneration (Khan et al., 2017). These interactions are consistent with the established relationships between *APOE* ε4 and AD pathologies amyloid and tau. *APOE* ε4 is clearly associated with increased Aβ aggregation, most likely by reducing the clearance of Aβ from the brain and increasing its production (Donahue and Johanson, 2008; Castellano et al., 2011; Wahrle et al., 2007; Mahley et al., 2006). It has also been reported that *APOE* ε4 carriers have increased levels of tau in the MTL (Jack et al., 2020; Ossenkoppele et al., 2016).

Our finding of positive correlations between Aβ aggregation and CBF in hypertensive individuals was the opposite of the interaction effect we expected hypertension to have, but

medRxiv preprint doi: https://doi.org/10.1101/2022.09.27.22280379; this version posted September 27, 2022. The copyright holder for this preprint (which was not certified by peer review) is the author/funder, who has granted medRxiv a license to display the preprint in perpetuity. All rights reserved. No reuse allowed without permission.

previous findings of positive associations between Aβ pathology and CBF in nondemented older individuals suggest that this finding could be meaningful. To our knowledge, this is the first report of such an interaction. Not only does this suggest that hypertension status may alter the interpretation of altered CBF as a biomarker, but it also suggests that cerebral vascular function is differentially affected by AD pathology in older adults with and without cardiovascular risk factors during preclinical stages of disease. The direction of the interaction was not expected; individuals with the risk factor of hypertension seemed to have more of a compensatory response (increased CBF) to Aβ pathology. This may suggest that the combined presence of risk factors and pathologies does not always favor loss of function in early disease stages. There is not yet a standard time course of when compensation fails to compensate, and it likely differs for each individual based on comorbidities, cardiovascular health, lifestyle choices like diet and exercise, and demographic, genetic, and environmental variables. Another possible reason that our findings were different than expected is because we defined hypertension as presence or absence of the condition at the time of imaging, but midlife hypertension confers the greatest risk for AD in old age (Lennon et al., 2021). It has also been reported that hypotension in old age, especially following midlife hypertension, is a risk factor for AD as well (Dickstein et al., 2010). As shown by the diverse findings reported in the literature, the relationship between amyloid pathology and CBF in older adults on the AD spectrum is very complex.

Surprisingly, we did not find an interaction effect of hypertension and tau on CBF or of *APOE* ε4 and either PET metric on CBF. It could be that hypertension and Aβ have relatively more independent effects on the cerebral vasculature than the other risk factor and pathology pairs. In support of this, we did find correlations between global cortical amyloid and *APOE* ε4 and between MTL tau and hypertension status in this sample. This is also in agreement with the

medRxiv preprint doi: https://doi.org/10.1101/2022.09.27.22280379; this version posted September 27, 2022. The copyright holder for this preprint (which was not certified by peer review) is the author/funder, who has granted medRxiv a license to display the preprint in perpetuity. All rights reserved. No reuse allowed without permission.

two-hit hypothesis of AD, in which cardiovascular risk and Aβ aggregation culminate to initiate and propagate the pathological processes in AD. At a more liberal statistical significance level, we did find brain regions with *APOE* ε4 by Aβ and tau interaction effects on CBF. With larger sample sizes, these interactions may prove to be meaningful. It is also possible that these interactions would be detectable and meaningful during later disease stages but not in preclinical stages.

This study was limited by its modest sample size. Some regions of associations between voxel-wise CBF and PET biomarkers did not reach statistical significance, and a larger sample size could have led to more statistically significant results suggesting a clearer picture of correlative patterns. Future studies should use larger sample sizes of individuals with preclinical AD so that statistical power is adequate to elucidate the complex relationships between CBF, amyloid, tau, and other AD-related pathologies. Our sample was also homogenous in terms of ethnoracial and educational backgrounds, and it will be important to utilize diverse samples in future studies. Additionally, we used global cortical Centiloid and MTL tau SUVR as our metrics of PET imaging. It would be ideal to retain the spatial information in both the PET and ASL images in order to determine areas of spatial overlap between AD pathologies and altered CBF. Finally, we defined hypertension by self-report rather than by a threshold blood pressure at the time of scanning, and some hypertensive individuals were taking antihypertensive medications. The addition of blood pressure and use of antihypertensives in our models did not change the results, but future studies with a narrower definition of hypertension may be beneficial.

4.1 Conclusions

medRxiv preprint doi: https://doi.org/10.1101/2022.09.27.22280379; this version posted September 27, 2022. The copyright holder for this preprint (which was not certified by peer review) is the author/funder, who has granted medRxiv a license to display the preprint in perpetuity. All rights reserved. No reuse allowed without permission.

Our findings suggest that MTL tau pathology is associated with decreased MTL CBF in older adults. They also suggest a positive interaction of amyloid pathology and hypertension status on occipital CBF; there may be a complex relationship between amyloid pathology and CBF that depends partially on cardiovascular health. Altered CBF is likely both an instigator and an outcome of increased amyloid and tau pathology, and these and other factors interact both spatially and temporally in the environment of an at-risk brain. CBF can be used as a potential biomarker in future studies to identify those at risk so that they can enter clinical trials and/or receive treatment, track disease progression in both treated and untreated individuals, and perhaps help elucidate the complex mechanisms that initiate AD and drive its progression.

medRxiv preprint doi: https://doi.org/10.1101/2022.09.27.22280379; this version posted September 27, 2022. The copyright holder for this preprint (which was not certified by peer review) is the author/funder, who has granted medRxiv a license to display the preprint in perpetuity. All rights reserved. No reuse allowed without permission.

Table 1. Demographic and clinical variables by diagnostic group.

	All (n=78)	CN (n=30)	SCD (n=25)	MCI (n=23)	Group Comparison *p*
Age	71.71 ± 6.78	71.13 ± 6.53	71.00 ± 7.12	73.22 ± 6.78	0.448
GM Volume (mm^3)	569,769 ± 59,277	576,393 ± 57,148	566,463 ± 63,286	564,723 ± 59,372	0.739
Hypertension	52.6%	26.7%	80.0%	56.5%	<0.001* SCD > MCI > CN
Sex (F)	65.4%	80.0%	64.0%	47.8%	0.050* CN > SCD > MCI
APOE ε4 positive	43.6%	46.7%	32.0%	52.2%	0.338
Amyloid PET (Centiloid)	19.41 ± 32.12	10.91 ± 26.13	11.10 ± 24.49	39.54 ± 38.16	0.001* MCI > CN&SCD
Tau PET (SUVR)	1.11 ± 0.11	1.09 ± 0.07	1.09 ± 0.08	1.15 ± 0.16	0.110

PET: positron emission tomography, CN: cognitively normal, SCD: subjective cognitive decline, MCI: mild cognitive impairment, GM: gray matter, APOE: apoliprotein E, CBF: cerebral blood flow, SUVR: standardized uptake value ratio

Table 2. Correlation of age and hypertension status with lobar CBF.

	Independent Variable retained in Model	Standardized Coefficient (β)	*t*	*p*
Frontal	Age	−0.335	−3.312	0.001
	Hypertension Status	−0.326	−3.221	0.002
Limbic	Age	−0.320	−3.033	0.003
	Hypertension Status	−0.239	−2.265	0.026
Parietal	Age	−0.284	−2.691	0.009
	Hypertension Status	−0.281	−2.671	0.009
Temporal	Age	−0.331	−3.199	0.002
	Hypertension Status	−0.277	−2.677	0.009
Occipital	Age	−0.313	−2.982	0.004
	Hypertension Status	−0.258	−2.453	0.016

Table 3. Regions of negative association between age and voxel-wise CBF. Peak effects reported in MNI coordinates (mm).

k	ROI	x	y	z	Brodmann area	*t*	Uncorrected cluster-wise *p*
804	left primary auditory	−50	−14	8	41	5.15	<0.001
	left superior temporal	−56	12	−6	22	4.43	
	left supramarginal	−48	−24	12	40	4.15	
	left insula	−38	−20	−4	13	3.87	
	left temporal pole	−42	12	−20	38	3.83	
	left superior temporal	−50	4	−4	22	3.82	
	left caudate	−36	−26	−8	N/A	3.81	
	left superior temporal	−42	−12	−6	22	3.72	
	left primary sensory	−60	−18	10	1	3.59	
	left temporal pole	−38	16	−24	38	3.58	
	left supramarginal	−44	−34	18	40	3.46	
154	left dorsal ACC	−4	42	2	32	4.45	0.022
	right orbital frontal	0	40	−8	11	3.64	

medRxiv preprint doi: https://doi.org/10.1101/2022.09.27.22280379; this version posted September 27, 2022. The copyright holder for this preprint (which was not certified by peer review) is the author/funder, who has granted medRxiv a license to display the preprint in perpetuity. All rights reserved. No reuse allowed without permission.

	right anterior PFC	8	48	−2	10	3.58	
338	right thalamus	6	−4	4	N/A	4.42	0.002
	right caudate	8	8	10	N/A	4.36	
	left thalamus	−4	−4	4	N/A	4.22	
	right caudate	10	22	0	N/A	3.64	
458	right primary visual	18	−84	12	17	4.35	<0.001
	right visual association	20	−68	34	19	3.98	
	right secondary visual	10	−98	12	18	3.62	
	right visual association	22	−78	28	19	3.50	
252	right temporal pole	30	20	−42	38	4.35	0.005
261	left amygdala	−14	−2	−18	N/A	4.32	0.005
109	right pars opercularis	40	20	14	44	4.27	0.049
	right pars triangularis	36	28	8	45	3.49	
625	right insula	42	−8	−8	13	4.20	<0.001
	right superior temporal	44	−42	10	22	4.00	
	right primary sensory	46	−16	12	1	3.98	
	right supramarginal	44	−32	16	40	3.91	
	right insula	40	2	−12	13	3.89	
	right hippocampus	36	−14	−22	N/A	3.69	
	right insula	40	−8	8	13	3.59	
	right primary auditory	38	−20	6	41	3.55	
	right insula	40	−18	2	13	3.45	
	right parahippocampal	36	−14	−34	36	3.34	
181	right pre and supplementary motor	38	−18	60	6	3.82	0.015
	right pre and supplementary motor	26	−16	62	6	3.69	

ROI: region of interest, PFC: prefrontal cortex, ACC: anterior cingulate cortex

Table 4. Regions of negative association between hypertension and voxel-wise CBF. p<0.001; k>50. Peak effects reported in MNI coordinates (mm).

k	ROI	x	y	z	Brodmann area	*t*	Uncorrected cluster-wise *p*
1222	right frontal eye fields	42	22	48	8	4.67	**<0.001**
	right frontal eye fields	36	8	56	8	4.60	
	right dorsolateral PFC	48	24	36	9	4.15	
	right pre and supplementary motor	24	10	62	6	3.77	
	right frontal eye fields	28	28	48	8	4.43	
	right pre and supplementary motor	28	0	64	6	3.90	

medRxiv preprint doi: https://doi.org/10.1101/2022.09.27.22280379; this version posted September 27, 2022. The copyright holder for this preprint (which was not certified by peer review) is the author/funder, who has granted medRxiv a license to display the preprint in perpetuity. All rights reserved. No reuse allowed without permission.

	right pre and supplementary motor	32	−4	60	6	3.79	
	right dorsolateral PFC	40	36	36	9	3.88	
	right dorsolateral PFC	44	36	28	9	3.47	
	right anterior PFC	18	58	24	10	4.07	
	right dorsolateral PFC	30	50	28	9	4.04	
	right dorsolateral PFC	24	44	38	9	3.90	
	right pre and supplementary motor	20	22	56	6	3.41	
700	left dorsolateral PFC	−12	52	34	9	4.26	<0.001
	left dorsolateral PFC	−4	50	36	9	4.16	
	left dorsolateral PFC	−22	46	34	9	4.72	
	left frontal eye fields	−12	46	40	8	4.04	
	left dorsolateral PFC	−26	40	36	9	3.92	
	right dorsolateral PFC	4	50	34	9	3.84	
	left pre and supplementary motor	−20	18	58	6	3.41	
	right dorsolateral PFC	12	48	42	9	3.38	
	left frontal eye fields	−18	32	52	8	4.14	
	left anterior PFC	−28	50	28	10	4.15	
	left frontal eye fields	−22	24	52	8	3.81	
	left frontal eye fields	−8	40	48	8	3.99	
	left frontal eye fields	−24	30	44	8	4.05	
706	left dorsolateral PFC	−46	24	34	9	4.63	<0.001
	left frontal eye fields	−32	18	54	8	4.48	
	left pre and supplementary motor	−32	6	60	6	4.26	
	left pre and supplementary motor	−38	0	56	6	4.06	
	left dorsolateral PFC	−36	34	36	9	4.00	

medRxiv preprint doi: https://doi.org/10.1101/2022.09.27.22280379; this version posted September 27, 2022. The copyright holder for this preprint (which was not certified by peer review) is the author/funder, who has granted medRxiv a license to display the preprint in perpetuity. All rights reserved. No reuse allowed without permission.

	left pre and supplementary motor	−18	−8	70	6	3.89	
	left pre and supplementary motor	−46	4	48	6	3.85	
	left pre and supplementary motor	−24	−4	66	6	3.85	
	left pre and supplementary motor	−32	8	58	6	3.62	
	left frontal eye fields	−42	10	38	8	3.39	
132	left temporal pole	−40	6	−38	38	4.29	0.031
	left temporal pole	−34	16	−34	38	3.63	
211	left pars orbitalis	−24	28	−12	47	4.43	0.009
	left orbital frontal	−22	38	−12	11	4.02	
111	right pre and supplementary motor	4	12	58	6	3.76	0.045
	right frontal eye fields	6	22	50	8	4.13	
178	right ventral anterior cingulate	2	−20	38	24	4.17	0.014
	left dorsal PCC	−2	−30	40	31	3.34	
122	right temporal pole	48	14	−30	38	4.06	0.037
	right temporal pole	42	14	−40	38	3.83	
	right temporal pole	56	12	−18	38	3.24	

ROI: region of interest, PFC: prefrontal cortex, PCC: posterior cingulate cortex

Table 5. Negative correlations between voxel-wise CBF and MTL tau SUVR. p<0.001; k>50. Peak effects reported in MNI coordinates (mm).

k	ROI	x	y	z	Brodmann area	*t*	Uncorrected cluster-wise *p*
123	left parahippocampal gyrus	−22	−22	−20	36	4.63	0.037
	left hippocampus	−14	−12	−18	N/A	3.60	

ROI: region of interest, MTL: medial temporal lobe, SUVR: standardized uptake value ratio

Table 6. Amyloid positivity by hypertension status interaction effect on voxel-wise CBF. p<0.001; k>50. Peak effects reported in MNI coordinates (mm).

k	ROI	x	y	z	Brodmann area	*F*	Uncorrected cluster-wise

medRxiv preprint doi: https://doi.org/10.1101/2022.09.27.22280379; this version posted September 27, 2022. The copyright holder for this preprint (which was not certified by peer review) is the author/funder, who has granted medRxiv a license to display the preprint in perpetuity. All rights reserved. No reuse allowed without permission.

							p
101	left visual motor	−26	−54	38	7	18.57	0.029

ROI: region of interest

medRxiv preprint doi: https://doi.org/10.1101/2022.09.27.22280379; this version posted September 27, 2022. The copyright holder for this preprint (which was not certified by peer review) is the author/funder, who has granted medRxiv a license to display the preprint in perpetuity. All rights reserved. No reuse allowed without permission.

Figure 1. Negative correlations between voxel-wise CBF and age (A & B) and hypertension status (C & D). Covariates are age (in the hypertension analysis), sex, and total gray matter volume. Illustrated at p 0.001, k 50.

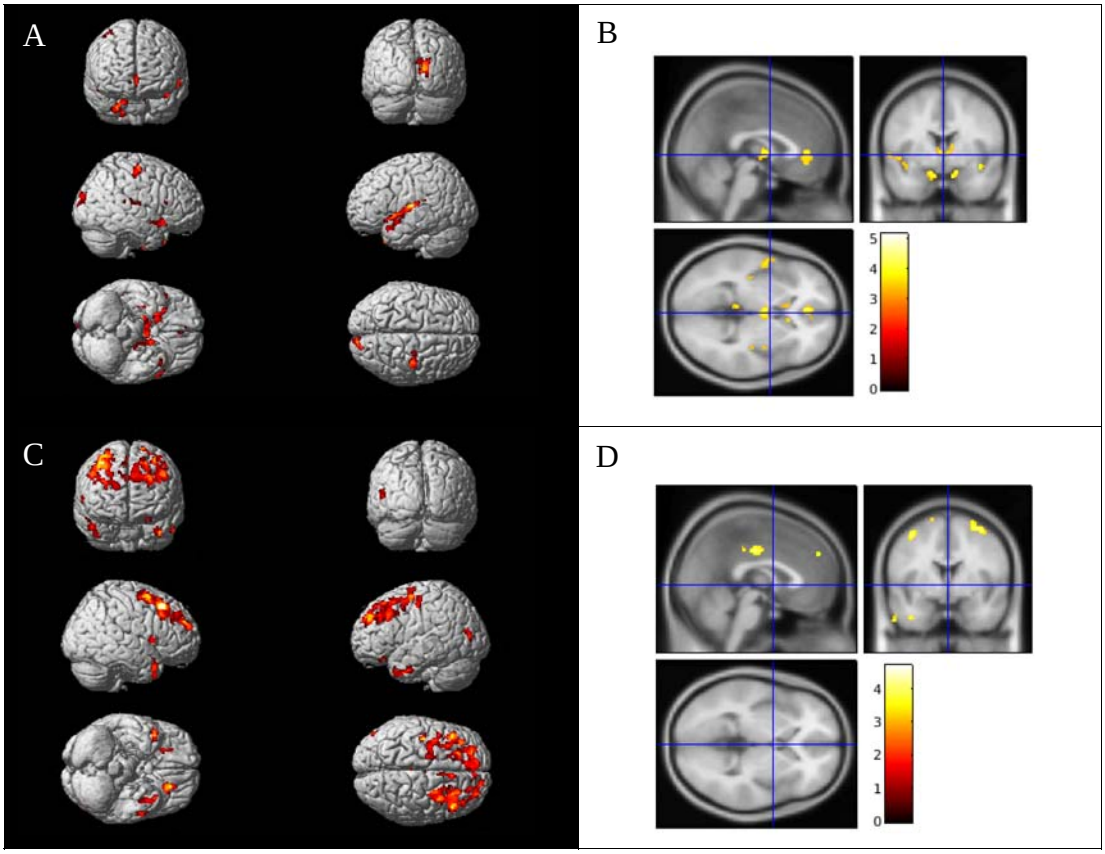

medRxiv preprint doi: https://doi.org/10.1101/2022.09.27.22280379; this version posted September 27, 2022. The copyright holder for this preprint (which was not certified by peer review) is the author/funder, who has granted medRxiv a license to display the preprint in perpetuity. All rights reserved. No reuse allowed without permission.

Figure 2. Voxel-wise CBF rendering (A) and beta maps (B-D) of negative correlations between voxel-wise CBF and MTL tau SUVR. Parahippocampal/hippocampal CBF are lower in those with increased MTL tau. Age, sex and total gray matter volume were the covariates. Rendering (A) displayed at p 0.001, k 50.

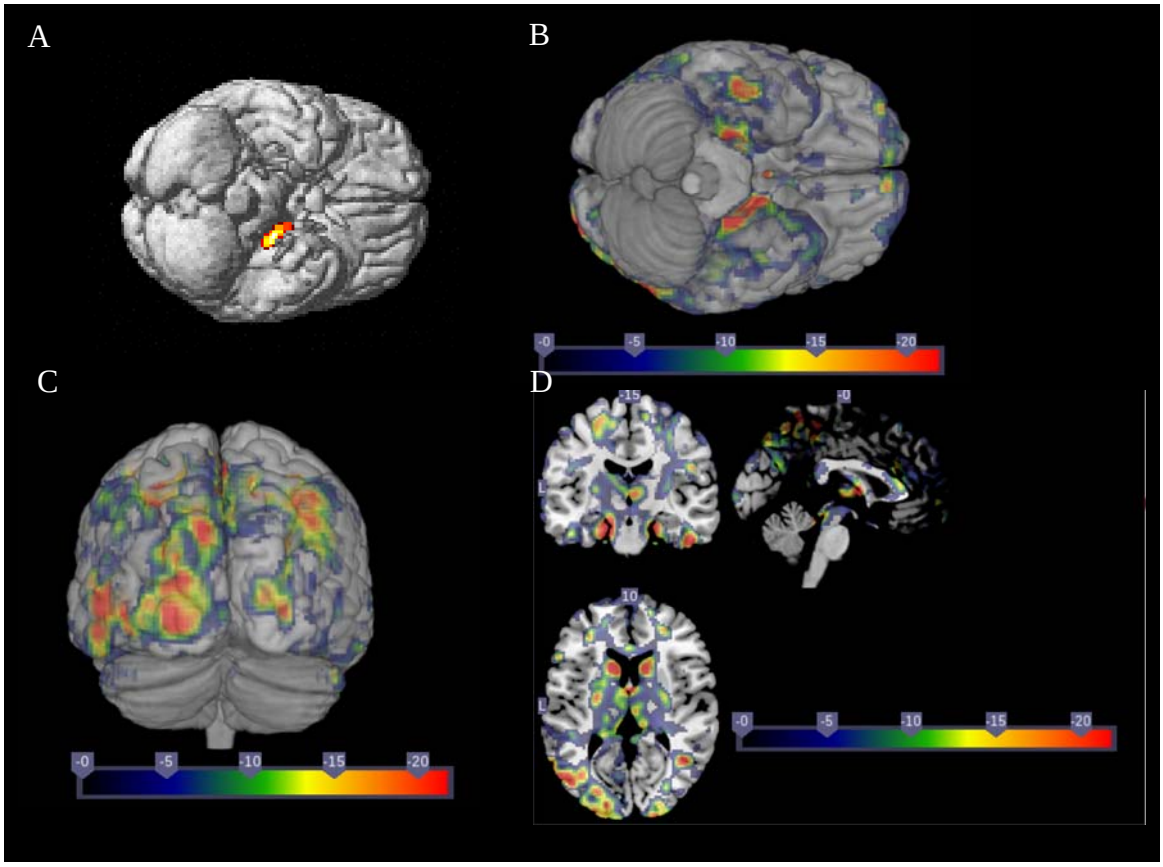

medRxiv preprint doi: https://doi.org/10.1101/2022.09.27.22280379; this version posted September 27, 2022. The copyright holder for this preprint (which was not certified by peer review) is the author/funder, who has granted medRxiv a license to display the preprint in perpetuity. All rights reserved. No reuse allowed without permission.

Figure 3. Scatterplot of negative correlations between voxel-wise CBF and MTL tau SUVR. Parahippocampal/hippocampal CBF are from the significant cluster in the voxel-wise analysis. Blue = CN, green = SCD, red = MCI. R^2=0.256.

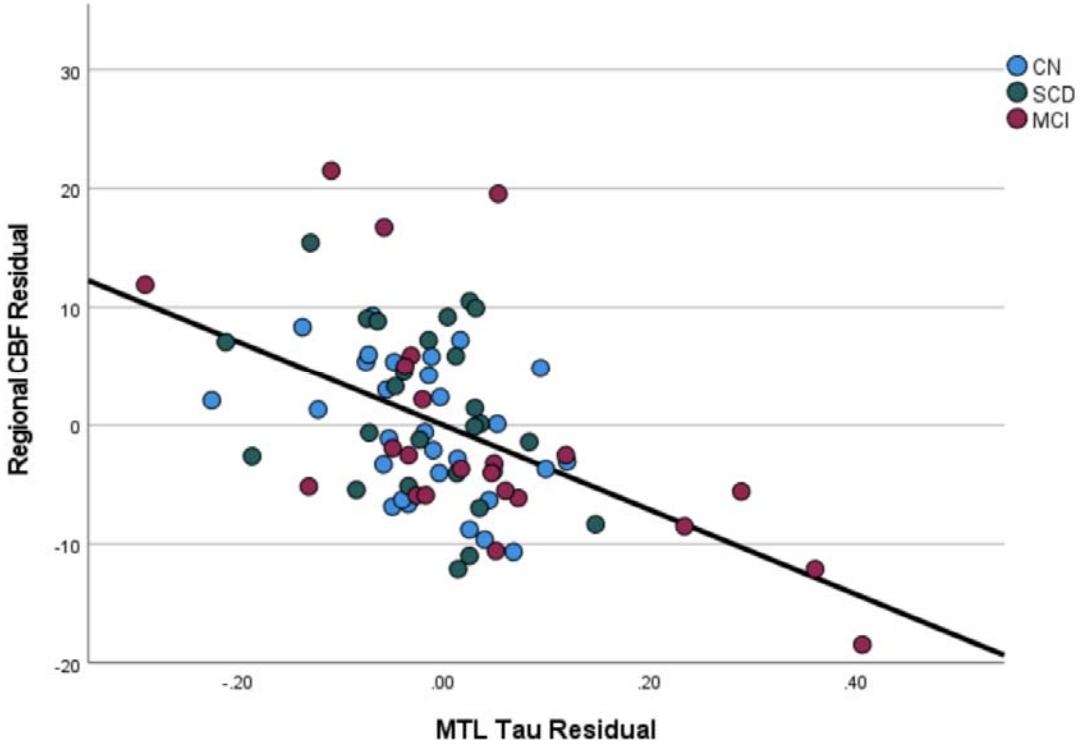

medRxiv preprint doi: https://doi.org/10.1101/2022.09.27.22280379; this version posted September 27, 2022. The copyright holder for this preprint (which was not certified by peer review) is the author/funder, who has granted medRxiv a license to display the preprint in perpetuity. All rights reserved. No reuse allowed without permission.

Figure 4. Voxel-wise CBF rendering (A) and beta maps (B-D) of the amyloid positivity by hypertension status effect in parietal, temporoparietal, temporal, and occipital regions. Age, sex and total gray matter volume were the model covariates. Rendering (A) displayed at p 0.001, k 50.

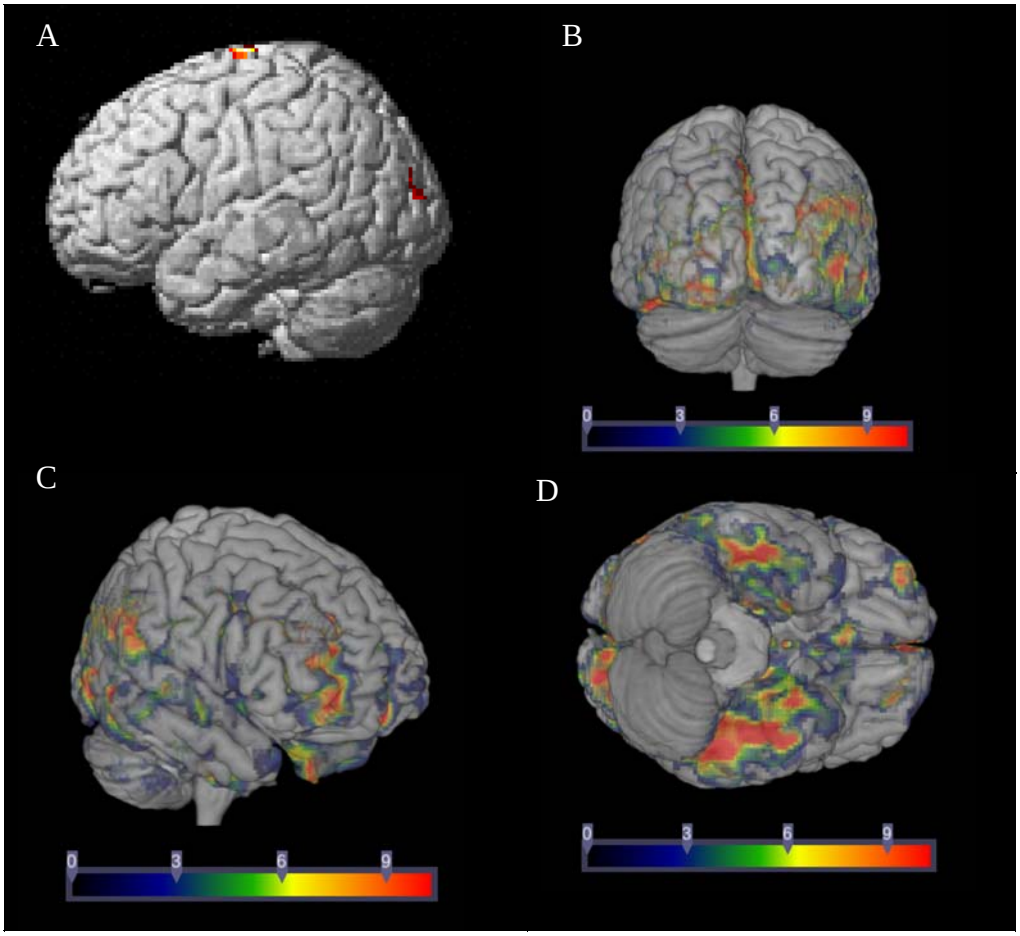

medRxiv preprint doi: https://doi.org/10.1101/2022.09.27.22280379; this version posted September 27, 2022. The copyright holder for this preprint (which was not certified by peer review) is the author/funder, who has granted medRxiv a license to display the preprint in perpetuity. All rights reserved. No reuse allowed without permission.

Figure 5. Interaction effect of global cortical Centiloid by hypertension status in visual motor and supramarginal CBF as defined by a significant cluster in the voxel-wise interaction analysis. In visual motor and supramarginal regions, CBF is positively associated with global cortical Centiloid in hypertensive individuals and negatively associated with global cortical Centiloid in normotensive individuals. Orange = individuals with hypertension, blue = individuals without hypertension.

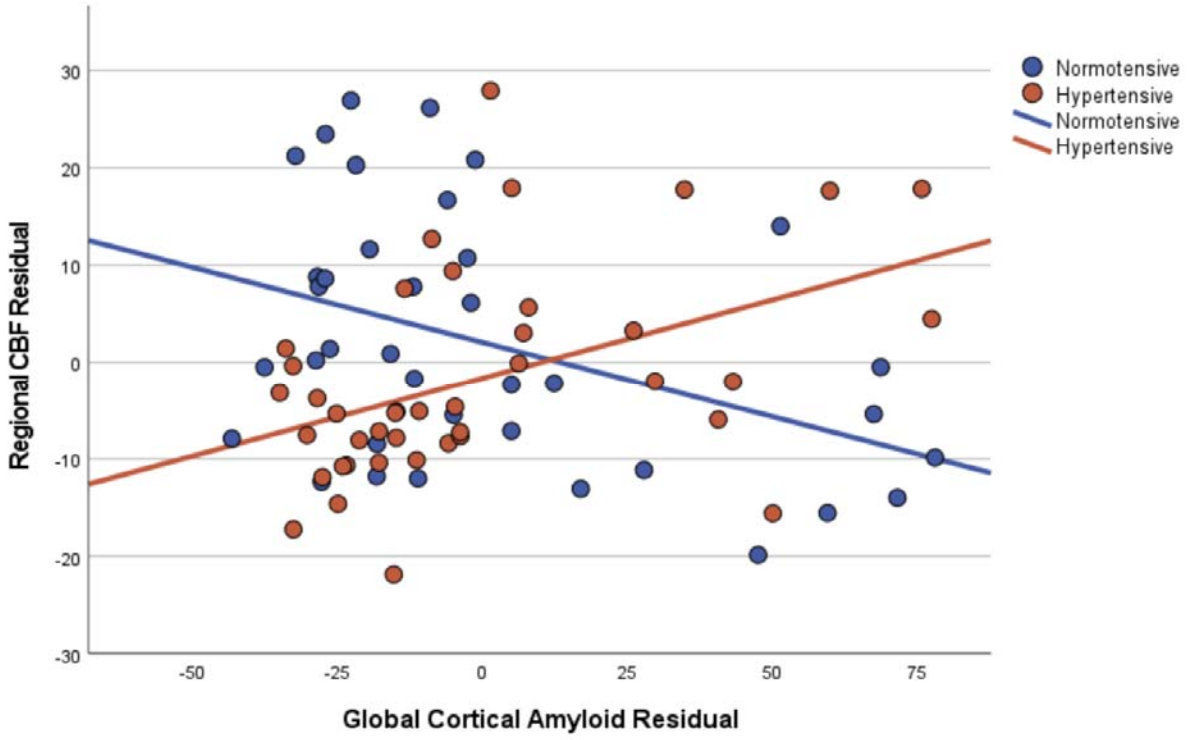

medRxiv preprint doi: https://doi.org/10.1101/2022.09.27.22280379; this version posted September 27, 2022. The copyright holder for this preprint (which was not certified by peer review) is the author/funder, who has granted medRxiv a license to display the preprint in perpetuity. All rights reserved. No reuse allowed without permission.

Acknowledgements:

John D. West, MSEng, Indiana University School of Medicine, played a primary role in optimizing and automating the pCASL processing pipeline, and the authors are grateful for his contributions to this research which we dedicate to his memory. We are grateful to the research participants and their families without whose generosity and commitment this study would not have been possible.

Declarations of Interest:

Dr. Apostolova receives support in the form of consulting fees from Biogen, Two Labs, IQVIA, NIH, Florida Department of Health, NIH Biobank, Eli Lilly, GE Healthcare, and Eisai; in the form of payment for lectures, etc. from AAN, MillerMed, AiSM, and Health and Hospitality; and in the form of travel and meeting support from Alzheimer's Association. She also participates on Data Safety Monitoring or Advisory boards for IQVIA, NIA R01 AG061111, UAB Nathan Shock Center, and New Mexico Exploratory ADRC; in leadership roles for Medical Science Council Alzheimer Association Greater IN Chapter, Alzheimer Association Science Program Committee, and FDA PCNS Advisory Committee; stock or stock options Cassava Neurosciences and Golden Seeds, and receipt of materials, etc. from AVID Pharmaceuticals, Life Molecular Imaging, and Roche Diagnostics.

Dr. Saykin has received support for consultation to Bayer Oncology (Scientific Advisory Board), Eisai (Scientific Advisory Board), Siemens Medical Solutions USA, Inc. (Dementia Advisory Board), and Springer-Nature Publishing (Editorial Office Support as Editor-in-Chief, Brain Imaging and Behavior).

Dr. Wang has received book royalties from American Psychiatric Publishing, Inc., and consultant fees for serving on a Data Safety Monitoring Board.

Dr. Clark receives royalties for two UpToDate articles on aphasia and has done paid consulting for Eli Lilly and Company on the topic of amyloid scans.

Dr. Brosch discloses the following: AbbVie [Progressive supranuclear palsy]; AbbVie [Alzheimer disease]; Avanir [Alzheimer disease]; Biogen [Alzheimer disease]; Biogen [Prodromal or mild Alzheimer disease]; Dominantly Inherited Alzheimer Network [Alzheimer disease]; Eisai [Early Alzheimer disease]; Eisai [Dementia with Lewy bodies]; Eli Lilly [Alzheimer disease]; Eli Lilly [Parkinson disease dementia]; Genentech [Alzheimer disease]; Novartis [Alzheimer disease]; Roche [Alzheimer disease]; Suven [Alzheimer disease].

All other authors report no disclosures.

medRxiv preprint doi: https://doi.org/10.1101/2022.09.27.22280379; this version posted September 27, 2022. The copyright holder for this preprint (which was not certified by peer review) is the author/funder, who has granted medRxiv a license to display the preprint in perpetuity. All rights reserved. No reuse allowed without permission.

References:

1. 2021 Alzheimer's disease facts and figures. Alzheimers Dement 2021;17(3):327-406. Epub 2021/03/24. doi: 10.1002/alz.12328. PubMed PMID: 33756057.
2. Albrecht D, Isenberg AL, Stradford J, Monreal T, Sagare A, Pachicano M, Sweeney M, Toga A, Zlokovic B, Chui H, Joe E, Schneider L, Conti P, Jann K, Pa J. Associations between Vascular Function and Tau PET Are Associated with Global Cognition and Amyloid. J Neurosci 2020;40(44):8573-86. Epub 2020/10/14. doi: 10.1523/JNEUROSCI.1230-20.2020. PubMed PMID: 33046556; PubMed Central PMCID: PMCPMC7605425.
3. Alosco ML, Gunstad J, Jerskey BA, Xu X, Clark US, Hassenstab J, Cote DM, Walsh EG, Labbe DR, Hoge R, Cohen RA, Sweet LH. The adverse effects of reduced cerebral perfusion on cognition and brain structure in older adults with cardiovascular disease. Brain Behav 2013;3(6):626-36. Epub 2013/12/24. doi: 10.1002/brb3.171. PubMed PMID: 24363966; PubMed Central PMCID: PMCPMC3868168.
4. Alsop DC, Detre JA, Golay X, Gunther M, Hendrikse J, Hernandez-Garcia L, Lu H, MacIntosh BJ, Parkes LM, Smits M, van Osch MJ, Wang DJ, Wong EC, Zaharchuk G. Recommended implementation of arterial spin-labeled perfusion MRI for clinical applications: A consensus of the ISMRM perfusion study group and the European consortium for ASL in dementia. Magn Reson Med 2015;73(1):102-16. Epub 2014/04/10. doi: 10.1002/mrm.25197. PubMed PMID: 24715426; PubMed Central PMCID: PMCPMC4190138.
5. Alsop DC, Detre JA, Grossman M. Assessment of cerebral blood flow in Alzheimer's disease by spin-labeled magnetic resonance imaging. Ann Neurol 2000;47(1):93-100. Epub 2000/01/13. PubMed PMID: 10632106.
6. Ashford JW, Shih WJ, Coupal J, Shetty R, Schneider A, Cool C, Aleem A, Kiefer VH, Mendiondo MS, Schmitt FA. Single SPECT measures of cerebral cortical perfusion reflect time-index estimation of dementia severity in Alzheimer's disease. J Nucl Med 2000;41(1):57-64. Epub 2000/01/27. PubMed PMID: 10647605.
7. Beishon L, Haunton VJ, Panerai RB, Robinson TG. Cerebral Hemodynamics in Mild Cognitive Impairment: A Systematic Review. J Alzheimers Dis 2017;59(1):369-85. Epub 2017/07/04. doi: 10.3233/JAD-170181. PubMed PMID: 28671118.
8. Bell RD, Winkler EA, Singh I, Sagare AP, Deane R, Wu Z, Holtzman DM, Betsholtz C, Armulik A, Sallstrom J, Berk BC, Zlokovic BV. Apolipoprotein E controls cerebrovascular integrity via cyclophilin A. Nature 2012;485(7399):512-6. Epub 2012/05/25. doi: 10.1038/nature11087. PubMed PMID: 22622580; PubMed Central PMCID: PMCPMC4047116.
9. Bennett RE, Robbins AB, Hu M, Cao X, Betensky RA, Clark T, Das S, Hyman BT. Tau induces blood vessel abnormalities and angiogenesis-related gene expression in P301L transgenic mice and human Alzheimer's disease. Proc Natl Acad Sci U S A 2018;115(6):E1289-E98. Epub 2018/01/24. doi: 10.1073/pnas.1710329115. PubMed PMID: 29358399; PubMed Central PMCID: PMCPMC5819390.
10. Binnewijzend MA, Kuijer JP, Benedictus MR, van der Flier WM, Wink AM, Wattjes MP, van Berckel BN, Scheltens P, Barkhof F. Cerebral blood flow measured with 3D pseudocontinuous arterial spin-labeling MR imaging in Alzheimer disease and mild cognitive impairment: a marker for disease severity. Radiology 2013;267(1):221-30. Epub 2012/12/15. doi: 10.1148/radiol.12120928. PubMed PMID: 23238159.
11. Boles Ponto LL, Magnotta VA, Moser DJ, Duff KM, Schultz SK. Global cerebral blood flow in relation to cognitive performance and reserve in subjects with mild memory deficits. Mol Imaging Biol 2006;8(6):363-72. Epub 2006/10/19. doi: 10.1007/s11307-006-0066-z. PubMed PMID: 17048070.

medRxiv preprint doi: https://doi.org/10.1101/2022.09.27.22280379; this version posted September 27, 2022. The copyright holder for this preprint (which was not certified by peer review) is the author/funder, who has granted medRxiv a license to display the preprint in perpetuity. All rights reserved. No reuse allowed without permission.

12. Brett M, Anton J, Vlabregue R, Poline J. Region of interest analysis using an SPM toolbox [abstract]. Presented at the 8th International Conferance on Functional Mapping of the Human Brain, June 2-6, 2002, Sendai, Japan. Available on CD-ROM in NeuroImage, Vol 16, No 2, abstract 497.
13. Butcher TJ, Chumin EJ, West JD, Dzemidzic M, Yoder KK. Cerebral Blood Flow in the Salience Network of Individuals with Alcohol Use Disorder. Alcohol Alcohol 2021. Epub 2021/09/21. doi: 10.1093/alcalc/agab062. PubMed PMID: 34541599.
14. Castellano JM, Kim J, Stewart FR, Jiang H, DeMattos RB, Patterson BW, Fagan AM, Morris JC, Mawuenyega KG, Cruchaga C, Goate AM, Bales KR, Paul SM, Bateman RJ, Holtzman DM. Human apoE isoforms differentially regulate brain amyloid-beta peptide clearance. Sci Transl Med 2011;3(89):89ra57. Epub 2011/07/01. doi: 10.1126/scitranslmed.3002156. PubMed PMID: 21715678; PubMed Central PMCID: PMCPMC3192364.
15. Chan SL, Bishop N, Li Z, Cipolla MJ. Inhibition of PAI (Plasminogen Activator Inhibitor)-1 Improves Brain Collateral Perfusion and Injury After Acute Ischemic Stroke in Aged Hypertensive Rats. Stroke 2018;49(8):1969-76. Epub 2018/07/12. doi: 10.1161/STROKEAHA.118.022056. PubMed PMID: 29991657; PubMed Central PMCID: PMCPMC6202199.
16. Chen YJ, Rosario BL, Mowrey W, Laymon CM, Lu X, Lopez OL, Klunk WE, Lopresti BJ, Mathis CA, Price JC. Relative 11C-PiB Delivery as a Proxy of Relative CBF: Quantitative Evaluation Using Single-Session 15O-Water and 11C-PiB PET. J Nucl Med 2015;56(8):1199-205. Epub 2015/06/06. doi: 10.2967/jnumed.114.152405. PubMed PMID: 26045309; PubMed Central PMCID: PMCPMC4730871.
17. Codispoti KE, Beason-Held LL, Kraut MA, O'Brien RJ, Rudow G, Pletnikova O, Crain B, Troncoso JC, Resnick SM. Longitudinal brain activity changes in asymptomatic Alzheimer disease. Brain Behav 2012;2(3):221-30. Epub 2012/06/29. doi: 10.1002/brb3.47. PubMed PMID: 22741095; PubMed Central PMCID: PMCPMC3381626.
18. Congdon EE, Sigurdsson EM. Tau-targeting therapies for Alzheimer disease. Nat Rev Neurol 2018;14(7):399-415. Epub 2018/06/14. doi: 10.1038/s41582-018-0013-z. PubMed PMID: 29895964; PubMed Central PMCID: PMCPMC6463489.
19. Crous-Bou M, Minguillon C, Gramunt N, Molinuevo JL. Alzheimer's disease prevention: from risk factors to early intervention. Alzheimers Res Ther 2017;9(1):71. Epub 2017/09/14. doi: 10.1186/s13195-017-0297-z. PubMed PMID: 28899416; PubMed Central PMCID: PMCPMC5596480.
20. Dai W, Lopez OL, Carmichael OT, Becker JT, Kuller LH, Gach HM. Mild cognitive impairment and alzheimer disease: patterns of altered cerebral blood flow at MR imaging. Radiology 2009;250(3):856-66. Epub 2009/01/24. doi: 10.1148/radiol.2503080751. PubMed PMID: 19164119; PubMed Central PMCID: PMCPMC2680168.
21. de la Torre JC, Pappas BA, Prevot V, Emmerling MR, Mantione K, Fortin T, Watson MD, Stefano GB. Hippocampal nitric oxide upregulation precedes memory loss and A beta 1-40 accumulation after chronic brain hypoperfusion in rats. Neurol Res 2003;25(6):635-41. Epub 2003/09/25. doi: 10.1179/016164103101201931. PubMed PMID: 14503018.
22. Dickstein DL, Walsh J, Brautigam H, Stockton SD, Jr., Gandy S, Hof PR. Role of vascular risk factors and vascular dysfunction in Alzheimer's disease. Mt Sinai J Med 2010;77(1):82-102. Epub 2010/01/27. doi: 10.1002/msj.20155. PubMed PMID: 20101718; PubMed Central PMCID: PMCPMC2918901.
23. Donahue JE, Johanson CE. Apolipoprotein E, amyloid-beta, and blood-brain barrier permeability in Alzheimer disease. J Neuropathol Exp Neurol 2008;67(4):261-70. Epub 2008/04/02. doi: 10.1097/NEN.0b013e31816a0dc8. PubMed PMID: 18379441.

medRxiv preprint doi: https://doi.org/10.1101/2022.09.27.22280379; this version posted September 27, 2022. The copyright holder for this preprint (which was not certified by peer review) is the author/funder, who has granted medRxiv a license to display the preprint in perpetuity. All rights reserved. No reuse allowed without permission.

24. Faraco G, Park L, Zhou P, Luo W, Paul SM, Anrather J, Iadecola C. Hypertension enhances Abeta-induced neurovascular dysfunction, promotes beta-secretase activity, and leads to amyloidogenic processing of APP. J Cereb Blood Flow Metab 2016;36(1):241-52. Epub 2015/04/30. doi: 10.1038/jcbfm.2015.79. PubMed PMID: 25920959; PubMed Central PMCID: PMCPMC4758560.
25. Fazlollahi A, Calamante F, Liang X, Bourgeat P, Raniga P, Dore V, Fripp J, Ames D, Masters CL, Rowe CC, Connelly A, Villemagne VL, Salvado O, Australian Imaging B, Lifestyle Research G. Increased cerebral blood flow with increased amyloid burden in the preclinical phase of alzheimer's disease. J Magn Reson Imaging 2020;51(2):505-13. Epub 2019/05/31. doi: 10.1002/jmri.26810. PubMed PMID: 31145515.
26. Fischl B, Dale AM. Measuring the thickness of the human cerebral cortex from magnetic resonance images. Proc Natl Acad Sci U S A 2000;97(20):11050-5. Epub 2000/09/14. doi: 10.1073/pnas.200033797. PubMed PMID: 10984517; PubMed Central PMCID: PMCPMC27146.
27. Gomez-Isla T, Hollister R, West H, Mui S, Growdon JH, Petersen RC, Parisi JE, Hyman BT. Neuronal loss correlates with but exceeds neurofibrillary tangles in Alzheimer's disease. Ann Neurol 1997;41(1):17-24. Epub 1997/01/01. doi: 10.1002/ana.410410106. PubMed PMID: 9005861.
28. Gorelick PB. Risk factors for vascular dementia and Alzheimer disease. Stroke 2004;35(11 Suppl 1):2620-2. Epub 2004/09/18. doi: 10.1161/01.STR.0000143318.70292.47. PubMed PMID: 15375299.
29. Hardy JA, Higgins GA. Alzheimer's disease: the amyloid cascade hypothesis. Science 1992;256(5054):184-5. Epub 1992/04/10. doi: 10.1126/science.1566067. PubMed PMID: 1566067.
30. Hays CC, Zlatar ZZ, Meloy MJ, Osuna J, Liu TT, Galasko DR, Wierenga CE. Anterior Cingulate Structure and Perfusion is Associated with Cerebrospinal Fluid Tau among Cognitively Normal Older Adult APOEvarepsilon4 Carriers. J Alzheimers Dis 2020;73(1):87-101. Epub 2019/11/21. doi: 10.3233/JAD-190504. PubMed PMID: 31743999; PubMed Central PMCID: PMCPMC7310575.
31. Iadecola C. Neurovascular regulation in the normal brain and in Alzheimer's disease. Nat Rev Neurosci 2004;5(5):347-60. Epub 2004/04/22. doi: 10.1038/nrn1387. PubMed PMID: 15100718.
32. Jack CR, Wiste HJ, Weigand SD, Therneau TM, Lowe VJ, Knopman DS, Botha H, Graff-Radford J, Jones DT, Ferman TJ, Boeve BF, Kantarci K, Vemuri P, Mielke MM, Whitwell J, Josephs K, Schwarz CG, Senjem ML, Gunter JL, Petersen RC. Predicting future rates of tau accumulation on PET. Brain 2020;143(10):3136-50. Epub 2020/10/24. doi: 10.1093/brain/awaa248. PubMed PMID: 33094327; PubMed Central PMCID: PMCPMC7586089.
33. Jaworski T, Lechat B, Demedts D, Gielis L, Devijver H, Borghgraef P, Duimel H, Verheyen F, Kugler S, Van Leuven F. Dendritic degeneration, neurovascular defects, and inflammation precede neuronal loss in a mouse model for tau-mediated neurodegeneration. Am J Pathol 2011;179(4):2001-15. Epub 2011/08/16. doi: 10.1016/j.ajpath.2011.06.025. PubMed PMID: 21839061; PubMed Central PMCID: PMCPMC3181369.
34. Jessen F, Amariglio RE, van Boxtel M, Breteler M, Ceccaldi M, Chetelat G, Dubois B, Dufouil C, Ellis KA, van der Flier WM, Glodzik L, van Harten AC, de Leon MJ, McHugh P, Mielke MM, Molinuevo JL, Mosconi L, Osorio RS, Perrotin A, Petersen RC, Rabin LA, Rami L, Reisberg B, Rentz DM, Sachdev PS, de la Sayette V, Saykin AJ, Scheltens P, Shulman MB, Slavin MJ, Sperling RA, Stewart R, Uspenskaya O, Vellas B, Visser PJ, Wagner M, Subjective Cognitive Decline Initiative Working G. A conceptual framework for research on subjective cognitive decline in preclinical Alzheimer's disease. Alzheimers Dement 2014;10(6):844-52. Epub 2014/05/07. doi: 10.1016/j.jalz.2014.01.001. PubMed PMID: 24798886; PubMed Central PMCID: PMCPMC4317324.
35. Khan MB, Hoda MN, Vaibhav K, Giri S, Wang P, Waller JL, Ergul A, Dhandapani KM, Fagan SC, Hess DC. Remote ischemic postconditioning: harnessing endogenous protection in a murine model

medRxiv preprint doi: https://doi.org/10.1101/2022.09.27.22280379; this version posted September 27, 2022. The copyright holder for this preprint (which was not certified by peer review) is the author/funder, who has granted medRxiv a license to display the preprint in perpetuity. All rights reserved. No reuse allowed without permission.

of vascular cognitive impairment. Transl Stroke Res 2015;6(1):69-77. Epub 2014/10/30. doi: 10.1007/s12975-014-0374-6. PubMed PMID: 25351177; PubMed Central PMCID: PMCPMC4297613.
36. Khan W, Giampietro V, Banaschewski T, Barker GJ, Bokde AL, Buchel C, Conrod P, Flor H, Frouin V, Garavan H, Gowland P, Heinz A, Ittermann B, Lemaitre H, Nees F, Paus T, Pausova Z, Rietschel M, Smolka MN, Strohle A, Gallinat J, Vellas B, Soininen H, Kloszewska I, Tsolaki M, Mecocci P, Spenger C, Villemagne VL, Masters CL, Muehlboeck JS, Backman L, Fratiglioni L, Kalpouzos G, Wahlund LO, Schumann G, Lovestone S, Williams SC, Westman E, Simmons A, Alzheimer-s Disease Neuroimaging I, AddNeuroMed Consortium AIB, Lifestyle Study Research G, consortium I. A Multi-Cohort Study of ApoE varepsilon4 and Amyloid-beta Effects on the Hippocampus in Alzheimer's Disease. J Alzheimers Dis 2017;56(3):1159-74. Epub 2017/02/06. doi: 10.3233/JAD-161097. PubMed PMID: 28157104; PubMed Central PMCID: PMCPMC5302035.
37. Klohs J, Rudin M, Shimshek DR, Beckmann N. Imaging of cerebrovascular pathology in animal models of Alzheimer's disease. Front Aging Neurosci 2014;6:32. Epub 2014/03/25. doi: 10.3389/fnagi.2014.00032. PubMed PMID: 24659966; PubMed Central PMCID: PMCPMC3952109.
38. Korte N, Nortley R, Attwell D. Cerebral blood flow decrease as an early pathological mechanism in Alzheimer's disease. Acta Neuropathol 2020;140(6):793-810. Epub 2020/09/01. doi: 10.1007/s00401-020-02215-w. PubMed PMID: 32865691; PubMed Central PMCID: PMCPMC7666276.
39. Lennon MJ, Koncz R, Sachdev PS. Hypertension and Alzheimer's disease: is the picture any clearer? Curr Opin Psychiatry 2021;34(2):142-8. Epub 2021/01/05. doi: 10.1097/YCO.0000000000000684. PubMed PMID: 33395097.
40. Liang W, Zhang W, Zhao S, Li Q, Liang H, Ceng R. Altered expression of neurofilament 200 and amyloid-beta peptide (1-40) in a rat model of chronic cerebral hypoperfusion. Neurol Sci 2015;36(5):707-12. Epub 2014/12/03. doi: 10.1007/s10072-014-2014-z. PubMed PMID: 25452168.
41. Lourenco CF, Ledo A, Barbosa RM, Laranjinha J. Neurovascular uncoupling in the triple transgenic model of Alzheimer's disease: Impaired cerebral blood flow response to neuronal-derived nitric oxide signaling. Exp Neurol 2017;291:36-43. Epub 2017/02/06. doi: 10.1016/j.expneurol.2017.01.013. PubMed PMID: 28161255.
42. Lu L, Zheng X, Wang S, Tang C, Zhang Y, Yao G, Zeng J, Ge S, Wen H, Xu M, Guyatt G, Xu N. Anti-Abeta agents for mild to moderate Alzheimer's disease: systematic review and meta-analysis. J Neurol Neurosurg Psychiatry 2020;91(12):1316-24. Epub 2020/10/14. doi: 10.1136/jnnp-2020-323497. PubMed PMID: 33046560.
43. Mahley RW, Weisgraber KH, Huang Y. Apolipoprotein E4: a causative factor and therapeutic target in neuropathology, including Alzheimer's disease. Proc Natl Acad Sci U S A 2006;103(15):5644-51. Epub 2006/03/29. doi: 10.1073/pnas.0600549103. PubMed PMID: 16567625; PubMed Central PMCID: PMCPMC1414631.
44. Mattsson N, Tosun D, Insel PS, Simonson A, Jack CR, Jr., Beckett LA, Donohue M, Jagust W, Schuff N, Weiner MW, Alzheimer's Disease Neuroimaging I. Association of brain amyloid-beta with cerebral perfusion and structure in Alzheimer's disease and mild cognitive impairment. Brain 2014;137(Pt 5):1550-61. Epub 2014/03/15. doi: 10.1093/brain/awu043. PubMed PMID: 24625697; PubMed Central PMCID: PMCPMC3999717.
45. Michels L, Warnock G, Buck A, Macauda G, Leh SE, Kaelin AM, Riese F, Meyer R, O'Gorman R, Hock C, Kollias S, Gietl AF. Arterial spin labeling imaging reveals widespread and Abeta-independent reductions in cerebral blood flow in elderly apolipoprotein epsilon-4 carriers. J Cereb Blood Flow Metab 2016;36(3):581-95. Epub 2015/12/15. doi: 10.1177/0271678X15605847. PubMed PMID: 26661143; PubMed Central PMCID: PMCPMC4794091.

medRxiv preprint doi: https://doi.org/10.1101/2022.09.27.22280379; this version posted September 27, 2022. The copyright holder for this preprint (which was not certified by peer review) is the author/funder, who has granted medRxiv a license to display the preprint in perpetuity. All rights reserved. No reuse allowed without permission.

46. Mishra S, Gordon BA, Su Y, Christensen J, Friedrichsen K, Jackson K, Hornbeck R, Balota DA, Cairns NJ, Morris JC, Ances BM, Benzinger TLS. AV-1451 PET imaging of tau pathology in preclinical Alzheimer disease: Defining a summary measure. Neuroimage 2017;161:171-8. Epub 2017/08/02. doi: 10.1016/j.neuroimage.2017.07.050. PubMed PMID: 28756238; PubMed Central PMCID: PMCPMC5696044.
47. Niwa K, Carlson GA, Iadecola C. Exogenous A beta1-40 reproduces cerebrovascular alterations resulting from amyloid precursor protein overexpression in mice. J Cereb Blood Flow Metab 2000;20(12):1659-68. Epub 2000/12/29. doi: 10.1097/00004647-200012000-00005. PubMed PMID: 11129782.
48. Niwa K, Kazama K, Younkin L, Younkin SG, Carlson GA, Iadecola C. Cerebrovascular autoregulation is profoundly impaired in mice overexpressing amyloid precursor protein. Am J Physiol Heart Circ Physiol 2002;283(1):H315-23. Epub 2002/06/14. doi: 10.1152/ajpheart.00022.2002. PubMed PMID: 12063304.
49. Niwa K, Porter VA, Kazama K, Cornfield D, Carlson GA, Iadecola C. A beta-peptides enhance vasoconstriction in cerebral circulation. Am J Physiol Heart Circ Physiol 2001;281(6):H2417-24. Epub 2001/11/16. doi: 10.1152/ajpheart.2001.281.6.H2417. PubMed PMID: 11709407.
50. Nortley R, Korte N, Izquierdo P, Hirunpattarasilp C, Mishra A, Jaunmuktane Z, Kyrargyri V, Pfeiffer T, Khennouf L, Madry C, Gong H, Richard-Loendt A, Huang W, Saito T, Saido TC, Brandner S, Sethi H, Attwell D. Amyloid beta oligomers constrict human capillaries in Alzheimer's disease via signaling to pericytes. Science 2019;365(6450). Epub 2019/06/22. doi: 10.1126/science.aav9518. PubMed PMID: 31221773; PubMed Central PMCID: PMCPMC6658218.
51. Okamura N, Arai H, Maruyama M, Higuchi M, Matsui T, Tanji H, Seki T, Hirai H, Chiba H, Itoh M, Sasaki H. Combined Analysis of CSF Tau Levels and [(123)I]Iodoamphetamine SPECT in Mild Cognitive Impairment: Implications for a Novel Predictor of Alzheimer's Disease. Am J Psychiatry 2002;159(3):474-6. Epub 2002/03/01. doi: 10.1176/appi.ajp.159.3.474. PubMed PMID: 11870015.
52. Ossenkoppele R, Schonhaut DR, Scholl M, Lockhart SN, Ayakta N, Baker SL, O'Neil JP, Janabi M, Lazaris A, Cantwell A, Vogel J, Santos M, Miller ZA, Bettcher BM, Vossel KA, Kramer JH, Gorno-Tempini ML, Miller BL, Jagust WJ, Rabinovici GD. Tau PET patterns mirror clinical and neuroanatomical variability in Alzheimer's disease. Brain 2016;139(Pt 5):1551-67. Epub 2016/03/11. doi: 10.1093/brain/aww027. PubMed PMID: 26962052; PubMed Central PMCID: PMCPMC5006248.
53. Park L, Hochrainer K, Hattori Y, Ahn SJ, Anfray A, Wang G, Uekawa K, Seo J, Palfini V, Blanco I, Acosta D, Eliezer D, Zhou P, Anrather J, Iadecola C. Tau induces PSD95-neuronal NOS uncoupling and neurovascular dysfunction independent of neurodegeneration. Nat Neurosci 2020;23(9):1079-89. Epub 2020/08/12. doi: 10.1038/s41593-020-0686-7. PubMed PMID: 32778793; PubMed Central PMCID: PMCPMC7896353.
54. Raz L, Bhaskar K, Weaver J, Marini S, Zhang Q, Thompson JF, Espinoza C, Iqbal S, Maphis NM, Weston L, Sillerud LO, Caprihan A, Pesko JC, Erhardt EB, Rosenberg GA. Hypoxia promotes tau hyperphosphorylation with associated neuropathology in vascular dysfunction. Neurobiol Dis 2019;126:124-36. Epub 2018/07/17. doi: 10.1016/j.nbd.2018.07.009. PubMed PMID: 30010004; PubMed Central PMCID: PMCPMC6347559.
55. Risacher SL, West JD, Deardorff R, Gao S, Farlow MR, Brosch JR, Apostolova LG, McAllister TW, Wu YC, Jagust WJ, Landau SM, Weiner MW, Saykin AJ, Alzheimer's Disease Neuroimaging I. Head injury is associated with tau deposition on PET in MCI and AD patients. Alzheimers Dement (Amst) 2021;13(1):e12230. Epub 2021/09/02. doi: 10.1002/dad2.12230. PubMed PMID: 34466653; PubMed Central PMCID: PMCPMC8383323.

medRxiv preprint doi: https://doi.org/10.1101/2022.09.27.22280379; this version posted September 27, 2022. The copyright holder for this preprint (which was not certified by peer review) is the author/funder, who has granted medRxiv a license to display the preprint in perpetuity. All rights reserved. No reuse allowed without permission.

56. Rodell AB, O'Keefe G, Rowe CC, Villemagne VL, Gjedde A. Cerebral Blood Flow and Abeta-Amyloid Estimates by WARM Analysis of [(11)C]PiB Uptake Distinguish among and between Neurodegenerative Disorders and Aging. Front Aging Neurosci 2016;8:321. Epub 2017/01/27. doi: 10.3389/fnagi.2016.00321. PubMed PMID: 28123366; PubMed Central PMCID: PMCPMC5225115.
57. Rubinski A, Tosun D, Franzmeier N, Neitzel J, Frontzkowski L, Weiner M, Ewers M. Lower cerebral perfusion is associated with tau-PET in the entorhinal cortex across the Alzheimer's continuum. Neurobiol Aging 2021;102:111-8. Epub 2021/03/26. doi: 10.1016/j.neurobiolaging.2021.02.003. PubMed PMID: 33765424; PubMed Central PMCID: PMCPMC8205941.
58. Saykin AJ, Wishart HA, Rabin LA, Santulli RB, Flashman LA, West JD, McHugh TL, Mamourian AC. Older adults with cognitive complaints show brain atrophy similar to that of amnestic MCI. Neurology 2006;67(5):834-42. Epub 2006/09/13. doi: 10.1212/01.wnl.0000234032.77541.a2. PubMed PMID: 16966547; PubMed Central PMCID: PMCPMC3488276.
59. Schwarz AJ, Yu P, Miller BB, Shcherbinin S, Dickson J, Navitsky M, Joshi AD, Devous MD, Sr., Mintun MS. Regional profiles of the candidate tau PET ligand 18F-AV-1451 recapitulate key features of Braak histopathological stages. Brain 2016;139(Pt 5):1539-50. Epub 2016/03/05. doi: 10.1093/brain/aww023. PubMed PMID: 26936940.
60. Sojkova J, Beason-Held L, Zhou Y, An Y, Kraut MA, Ye W, Ferrucci L, Mathis CA, Klunk WE, Wong DF, Resnick SM. Longitudinal cerebral blood flow and amyloid deposition: an emerging pattern? J Nucl Med 2008;49(9):1465-71. Epub 2008/08/16. doi: 10.2967/jnumed.108.051946. PubMed PMID: 18703614; PubMed Central PMCID: PMCPMC2570023.
61. Solis E, Jr., Hascup KN, Hascup ER. Alzheimer's Disease: The Link Between Amyloid-beta and Neurovascular Dysfunction. J Alzheimers Dis 2020;76(4):1179-98. Epub 2020/07/01. doi: 10.3233/JAD-200473. PubMed PMID: 32597813; PubMed Central PMCID: PMCPMC7483596.
62. Stomrud E, Forsberg A, Hagerstrom D, Ryding E, Blennow K, Zetterberg H, Minthon L, Hansson O, Londos E. CSF biomarkers correlate with cerebral blood flow on SPECT in healthy elderly. Dement Geriatr Cogn Disord 2012;33(2-3):156-63. Epub 2012/06/23. doi: 10.1159/000338185. PubMed PMID: 22722670.
63. Swinford CG, Risacher SL, Wu Y, Apostolova LG, Gao S, Saykin AJ. Altered Cerebral Blood Flow in Older Adults with Alzheimer’s Disease: A Systematic Review. 2022. medRxiv doi: 10.1101/2022.03.24.22272916.
64. Takahashi M, Tada T, Nakamura T, Koyama K, Momose T. Efficacy and Limitations of rCBF-SPECT in the Diagnosis of Alzheimer's Disease With Amyloid-PET. Am J Alzheimers Dis Other Demen 2019;34(5):314-21. Epub 2019/04/11. doi: 10.1177/1533317519841192. PubMed PMID: 30966759; PubMed Central PMCID: PMCPMC6610554.
65. Tosun D, Joshi S, Weiner MW, the Alzheimer's Disease Neuroimaging I. Multimodal MRI-based Imputation of the Abeta+ in Early Mild Cognitive Impairment. Ann Clin Transl Neurol 2014;1(3):160-70. Epub 2014/04/15. doi: 10.1002/acn3.40. PubMed PMID: 24729983; PubMed Central PMCID: PMCPMC3981105.
66. Tosun D, Schuff N, Jagust W, Weiner MW, Alzheimer"s Disease Neuroimaging I. Discriminative Power of Arterial Spin Labeling Magnetic Resonance Imaging and 18F-Fluorodeoxyglucose Positron Emission Tomography Changes for Amyloid-beta-Positive Subjects in the Alzheimer's Disease Continuum. Neurodegener Dis 2016;16(1-2):87-94. Epub 2015/11/13. doi: 10.1159/000439257. PubMed PMID: 26560336.
67. Toth P, Tarantini S, Csiszar A, Ungvari Z. Functional vascular contributions to cognitive impairment and dementia: mechanisms and consequences of cerebral autoregulatory dysfunction, endothelial impairment, and neurovascular uncoupling in aging. Am J Physiol Heart Circ Physiol

medRxiv preprint doi: https://doi.org/10.1101/2022.09.27.22280379; this version posted September 27, 2022. The copyright holder for this preprint (which was not certified by peer review) is the author/funder, who has granted medRxiv a license to display the preprint in perpetuity. All rights reserved. No reuse allowed without permission.

2017;312(1):H1-H20. Epub 2016/10/30. doi: 10.1152/ajpheart.00581.2016. PubMed PMID: 27793855; PubMed Central PMCID: PMCPMC5283909.
68. Visser D, Wolters EE, Verfaillie SCJ, Coomans EM, Timmers T, Tuncel H, Reimand J, Boellaard R, Windhorst AD, Scheltens P, van der Flier WM, Ossenkoppele R, van Berckel BNM. Tau pathology and relative cerebral blood flow are independently associated with cognition in Alzheimer's disease. Eur J Nucl Med Mol Imaging 2020;47(13):3165-75. Epub 2020/05/29. doi: 10.1007/s00259-020-04831-w. PubMed PMID: 32462397; PubMed Central PMCID: PMCPMC7680306.
69. Wahrle SE, Shah AR, Fagan AM, Smemo S, Kauwe JS, Grupe A, Hinrichs A, Mayo K, Jiang H, Thal LJ, Goate AM, Holtzman DM. Apolipoprotein E levels in cerebrospinal fluid and the effects of ABCA1 polymorphisms. Mol Neurodegener 2007;2:7. Epub 2007/04/14. doi: 10.1186/1750-1326-2-7. PubMed PMID: 17430597; PubMed Central PMCID: PMCPMC1857699.
70. Wang J, Alsop DC, Song HK, Maldjian JA, Tang K, Salvucci AE, Detre JA. Arterial transit time imaging with flow encoding arterial spin tagging (FEAST). Magn Reson Med 2003;50(3):599-607. Epub 2003/08/27. doi: 10.1002/mrm.10559. PubMed PMID: 12939768.
71. Wang J, Peng G, Liu P, Tan X, Luo B, Alzheimer's Disease Neuroimaging I. Regulating effect of CBF on memory in cognitively normal older adults with different ApoE genotype: the Alzheimer's Disease Neuroimaging Initiative (ADNI). Cogn Neurodyn 2019;13(6):513-8. Epub 2019/11/20. doi: 10.1007/s11571-019-09536-x. PubMed PMID: 31741688; PubMed Central PMCID: PMCPMC6825072.
72. Wierenga CE, Hays CC, Zlatar ZZ. Cerebral blood flow measured by arterial spin labeling MRI as a preclinical marker of Alzheimer's disease. J Alzheimers Dis 2014;42 Suppl 4:S411-9. Epub 2014/08/28. doi: 10.3233/JAD-141467. PubMed PMID: 25159672; PubMed Central PMCID: PMCPMC5279221.
73. Wiesmann M, Zerbi V, Jansen D, Haast R, Lutjohann D, Broersen LM, Heerschap A, Kiliaan AJ. A Dietary Treatment Improves Cerebral Blood Flow and Brain Connectivity in Aging apoE4 Mice. Neural Plast 2016;2016:6846721. Epub 2016/04/02. doi: 10.1155/2016/6846721. PubMed PMID: 27034849; PubMed Central PMCID: PMCPMC4806294.
74. Zhang ZH, Fang XB, Xi GM, Li WC, Ling HY, Qu P. Calcitonin gene-related peptide enhances CREB phosphorylation and attenuates tau protein phosphorylation in rat brain during focal cerebral ischemia/reperfusion. Biomed Pharmacother 2010;64(6):430-6. Epub 2010/06/12. doi: 10.1016/j.biopha.2009.06.009. PubMed PMID: 20537498.
75. Zlatar ZZ, Bischoff-Grethe A, Hays CC, Liu TT, Meloy MJ, Rissman RA, Bondi MW, Wierenga CE. Higher Brain Perfusion May Not Support Memory Functions in Cognitively Normal Carriers of the ApoE epsilon4 Allele Compared to Non-Carriers. Front Aging Neurosci 2016;8:151. Epub 2016/07/23. doi: 10.3389/fnagi.2016.00151. PubMed PMID: 27445794; PubMed Central PMCID: PMCPMC4919360.
76. Zlokovic BV. Neurovascular pathways to neurodegeneration in Alzheimer's disease and other disorders. Nat Rev Neurosci 2011;12(12):723-38. Epub 2011/11/04. doi: 10.1038/nrn3114. PubMed PMID: 22048062; PubMed Central PMCID: PMCPMC4036520.